Ecological Indicators 98 (2019) 462–475

Contents lists available at ScienceDirect

Ecological Indicators

journal homepage: www.elsevier.com/locate/ecolind

Original Articles

Spatial-temporal changes in vegetation cover in a typical semi-humid and semi-arid region in China: Changing patterns, causes and implications

Saiyan Liu[a], Shengzhi Huang[a,*], Yangyang Xie[b], Hao Wang[c], Qiang Huang[a], Guoyong Leng[d], Pei Li[a], Lu Wang[a]

[a] State Key Laboratory Base of Eco-Hydraulic Engineering in Arid Area, Xi'an University of Technology, Xi'an 710048, China
[b] School of Hydrologic Energy and Power Engineering, Research Institute of Modern Rural Water Conservancy, Yangzhou 225009, China
[c] China Inst Hydropower & Water Resources, State Key Lab Simulat & Regulat Water Cycle River, Beijing 100038, China
[d] Environmental Change Institute, University of Oxford, Oxford OX1 3QY, UK

ARTICLE INFO

Keywords:
Vegetation cover
Soil moisture
Runoff
Sediment load
The Wei River Basin
The Loess Plateau

ABSTRACT

As a principal part of terrestrial ecological environment, vegetation is dominant in maintaining the function of terrestrial ecosystem. In order to systematically study the change patterns, causes, and implications of vegetation cover in a typical semi-humid and semi-arid region under changing environments, the Wei River Basin (WRB) was selected as the case study. Spatial-temporal changing patterns of vegetation cover in the WRB were firstly examined based on satellite-based Normalized Difference Vegetation Index (NDVI). Then, the underlying causes were studied by investigating the relationships among precipitation, temperature and soil moisture (SM) condition using the cross wavelet technique. Furthermore, implications of changing vegetation cover on runoff and sediment load were also analyzed. Results indicated that: (1) significant increasing trends of vegetation cover were detected at annual scale; and seasonal vegetation cover in the WRB is characterized with significant increasing trends in spring and autumn, while insignificant decreasing trend of summer vegetation cover in the upstream and midstream; (2) stationarity of annual NDVI is invalid with change points identified in all subregions of the WRB; (3) the correlations between annual NDVI series and precipitation, temperature and SM series demonstrate that significant increasing vegetation cover in the WRB are more influenced by temperature and SM condition than precipitation, anthropogenic factor however is also another reason for changing vegetation cover in the basin; and (4) statistically significant negative correlations between NDVI and runoff, sediment discharge imply that aside from human activities, increasing vegetation cover partially contributes to the reduction of runoff and sediment in the WRB. These findings are helpful for scientific assessment of ecological restoration projects, thereby facilitating local soil and water conservation.

1. Introduction

Terrestrial ecosystem is highly vulnerable to environmental changes (Chen et al., 2016, 2018; Zewdie et al., 2017), which has been severely affected by global climate change and the intensification of human activities in the past few decades (Piao et al., 2014; Bao et al., 2016; Wen et al., 2016; Meng et al., 2019). Hence, comprehensive study of long term terrestrial ecosystem changes is important for a better idea of sensitivity and vulnerability of ecosystem to environmental changes. Moreover, it is helpful for management of natural resources and development of adaptive strategies to changing environments (Gillespie et al., 2018). As a principal part of terrestrial ecological environment, vegetation is dominant in maintaining the function of terrestrial ecosystem (Jong et al., 2011; Cao et al., 2014). Affected by global warming and increasing anthropogenic pressures, there are notable changes in vegetation cover at global and regional scales in recent decades (Jong et al., 2011; Zhang et al., 2013; Piao et al., 2014; Pang et al., 2016; Huang et al., 2016; Wen et al., 2016). Therefore, vegetation cover is usually considered as a sensitive indicator of biological responses to environmental changes (Jong et al., 2011; Wen et al., 2016). Systemic investigation on dynamic changes in vegetation cover and the drivers thus has been a hot topic, which is conducive to monitor terrestrial ecosystem evolution, eco-environmental changes and to guide regional environmental management under changing environments (Zhang et al., 2013; Pang et al., 2016; Fang et al., 2017; Wen et al., 2016).

* Corresponding author at: State Key Laboratory of Eco-hydraulics in Northwest Arid Region of China, Xi'an University of Technology, Xi'an 710048, China.
E-mail address: huangshengzhi@xaut.edu.cn (S. Huang).

https://doi.org/10.1016/j.ecolind.2018.11.037
Received 6 July 2018; Received in revised form 3 October 2018; Accepted 13 November 2018

Over the past decades, satellite remote sensing provided a thriving perspective to monitor vegetation cover changes at various spatial and temporal scales in a repeatable manner (Wen et al., 2016). The satellite-based Normalized Difference Vegetation Index (NDVI), available since the early 1980s, has been the most widely used proxy of vegetation cover around the world (Begue et al., 2011; Chen et al., 2014a, b; Bao et al., 2016; Li et al., 2016; Wen et al., 2016). To date, many studies have focused on vegetation cover and their response to changing environments with the use of NDVI (Liu and Menzel, 2016). For example, on the global scale, Jong et al. (2011) found there was a significant greening (increasing NDVI) trend across western India, north-western Canada, Western Australia, Asia Minor and parts of the Sahel, whilst browning (decreasing NDVI) trend was observed in the tropical Africa and Indonesia/Oceania and in northern Argentina. At the regional scale, increasing trends have been detected in the monthly NDVI time series for all vegetation types in Southwest Germany which can be primarily attributed to temperature variation (Liu and Menzel, 2016). Based on biweekly NDVI dataset, Wang et al. (2003) claimed a significant increasing trend of vegetation in growing season in the central Great Plains of the USA, and precipitation is highly correlated with NDVI values during growing season and seven preceding months. In Southwestern Karst Region of China, Hou et al. (2015) discovered a significant increasing trend of NDVI in growing season, and claimed that the reduced temperature and solar radiation caused by the increase of precipitation may account for vegetation cover changes. Generally, these studies well advanced our knowledge of vegetation cover response to changing environments at different spatial and temporal scales. Nevertheless, there is no study comprehensively investigating the changing patterns, causes and implications of vegetation cover in a specific region, which is of important significance to monitor terrestrial ecosystem evolution under changing environments, especially for semi-humid and semi-arid region, like the Loess Plateau. The Loess Plateau is considered as the most severely eroded zone in the world, in which severe water loss and soil erosion have increased the fragility of the ecology (Reynolds et al., 2007; Li et al., 2016; Jia et al., 2017; Liu et al., 2018a). Due to changing climate and increasing human activities, it is essential to study vegetation cover variability in this region, along with exploring its causes and implications.

Drivers for vegetation cover variability are complex. They might be climatic factors, such as precipitation, temperature, soil moisture (SM) condition as well as human activities (e.g. Chen et al., 2014b; Hou et al., 2015; Liu and Menzel, 2016). However, previous studies tend to apply correlation coefficients (e.g. Pearson's correlation, linear correlation; Bao et al., 2016; Li et al., 2016) to investigate the relationships between vegetation coverage (indexed by NDVI) and climatic factors, which is too simple to reflect the changes or evolution of the relations between them (Liu et al., 2017). Hence, in this study we employed a new method called the cross wavelet analysis to fully examine their linkages in both time and frequency domains rather than simply calculating correlation coefficients. The cross wavelet analysis is a technique combining the cross spectrum analysis with wavelet transform (Torrence and Compo, 1998). Furthermore, it provides the distribution laws of the energy resonance and covariance of two time series in both time and frequency fields, thus being able to capture the nonlinear characteristics in their relationships (Torrence and Compo, 1998; Huang et al., 2017).

On the other hand, changes in vegetation cover has been well demonstrated to influence the regional hydrological cycle through regulating the surface energy balance and evapotranspiration (Begue et al., 2011; Zhang et al., 2011; Chen et al., 2014b; Bao et al., 2016; Wen et al., 2016; Li et al., 2016). Moreover, vegetation cover would directly or indirectly affect soil erosion processes (Lei et al., 2014; Duan et al., 2016). Specifically, vegetation cover could reduce the kinetic energy of raindrops; and the litter layer could protect soil surfaces (Zhang et al., 2015; Duan et al., 2016), increase soil surface roughness, impede overland flow and increase infiltrating time (Lei et al., 2014; Zhang et al., 2015; Duan et al., 2016). Consequently, streamflow and sediment load would be affected by changing vegetation cover. However, vegetation-induced changes in runoff and sediment load have not been well documented (Zheng, 2006; Li et al., 2016). Therefore, this study aims to explore the changing vegetation cover implications on runoff and sediment load, which helps to evaluate local soil and water conservation and ecological restoration projects.

Situated in southeastern part of the Loess Plateau, the Wei River Basin (WRB) is a typical semi-humid and semi-arid region in China (Guo et al., 2018; Liu et al., 2018b; Fang et al., 2019). As an eco-vulnerable and eco-sensitive zone (Chang et al., 2015; Huang et al., 2017), recent decades have witnessed severe environmental degradations in the basin. To tackle the serious environmental and ecological issues in the basin, Chinese government carried out a series of ecological restoration projects since the 1970s (Chang et al., 2015). Besides, climate change across the basin, including precipitation (Chang et al., 2015; Liu et al., 2017), temperature (Chang et al., 2015; Liu et al., 2018b), evaporation (Huang et al., 2014a; Fang et al., 2018) and drought (Huang et al., 2014b; Huang et al., 2015) have been well examined. However, little attention was paid to vegetation cover dynamics in the WRB, which constitutes the motivation of our study.

The main objectives of this study are: (1) to examine the changing patterns of vegetation cover across the WRB; (2) to explore the possible drivers of vegetation cover variations in terms of precipitation, temperature, SM condition and human activities; and (3) to investigate the possible implications of vegetation cover variations on runoff and sediment load.

2. Study area and data

2.1. Study area

As shown in Fig. 1, the WRB is located between 33.5° N-37.5° N and 103.5° E-110.5° E. It is the largest tributary of Yellow River Basin (YRB). Long-term average annual precipitation of the river is about 600 mm, and long-term average annual temperature ranges from 7.8 °C to 13.5 °C (Guo et al., 2018). Originating from the north side of the Niaoshu Mountains in the Gansu Province, the river flows through three provinces: Gansu, Ningxia, and Shaanxi. The drainage area of the WRB is 134,800 km^2, of which Gansu Province accounts for 44.1%, Ningxia Province 6.1%, Shaanxi Province 49.8% (Huang et al., 2014c). The main stream of the basin is 818 km, which can be divided into three sections: upper, middle and lower reaches. Their corresponding hydrological stations are the Linjiacun, Xianyang and Huaxian stations, respectively (Fig. 1B). There are two largest tributaries of the WRB, i.e. the Jing River Basin (JRB) and the Beiluo River Basin (BRB) with their corresponding hydrological stations are the Zhangjiashan and Zhuangtou stations, respectively. Notably, topography and geomorphological conditions in the river are complicated (Fig. 1A). Hence, to fully examine the spatial variation features of vegetation coverage across the WRB, the whole basin was divided into five sub-basins in this study. They are the upstream, midstream, downstream, the JRB, and the BRB (Fig. 1B).

2.2. Data

The following dataset were used in this study. NDVI data (1982–2010) was provided by NOAA's Advanced Very High Resolution Radiometer (AVHRR) (https://nex.nasa.gov/nex/projects/1349/). Daily temperature and precipitation of 21 meteorological stations (Table 1 and Fig. 1) were downloaded from China National Climatic Centre. In order to study the impacts of changing vegetation on runoff and sediment load, related dataset of five hydrological stations (Table 2 and Fig. 1) were collected from Yellow River Conservancy Commission. Besides, the gridded yearly SM data are simulated and obtained by the Variable Infiltration Capacity model. In addition, we also collected data

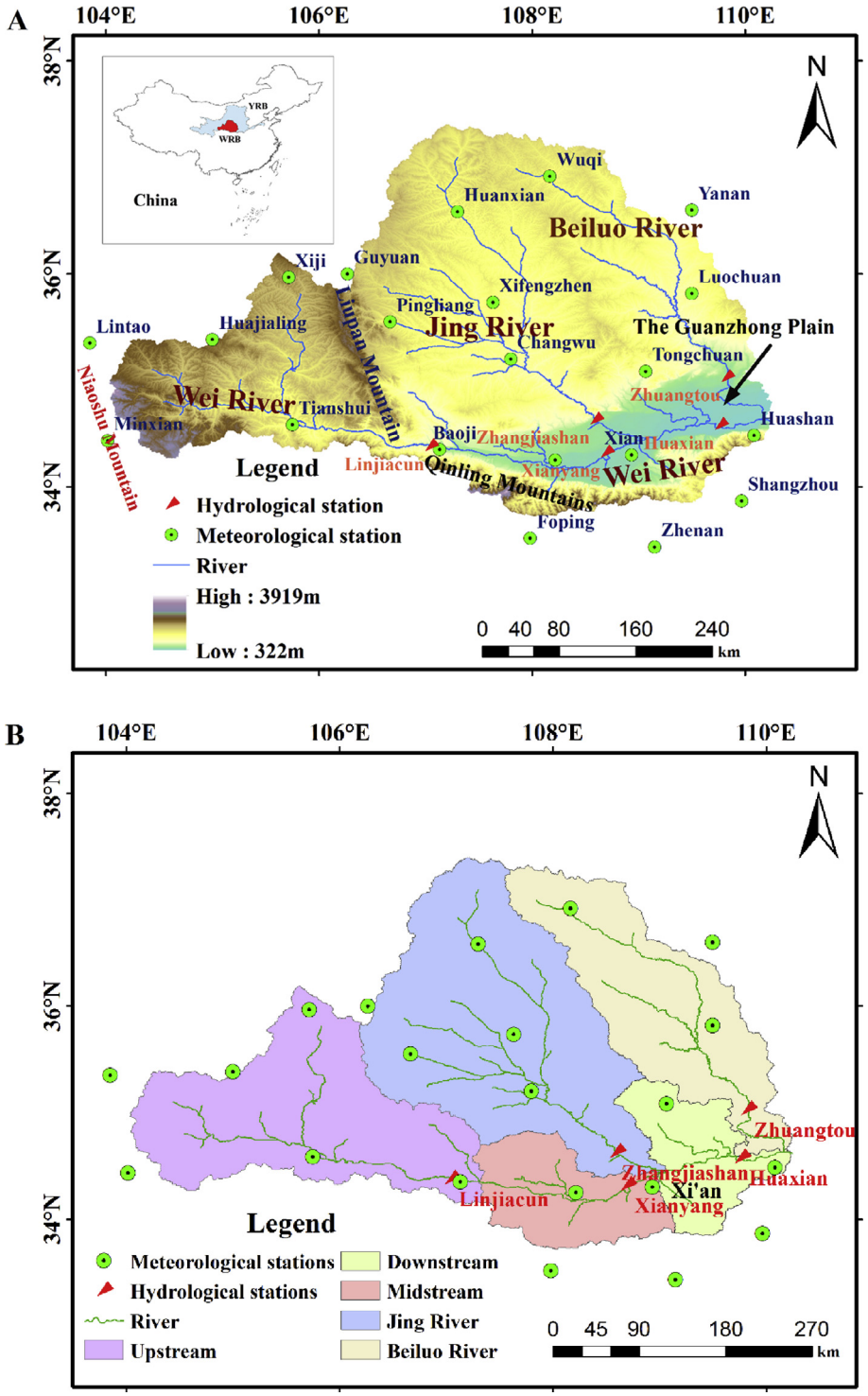

Fig. 1. Location of the WRB and relevant hydro-meteorological stations across the basin (A); and the five sub-basins of the WRB (B).

of different soil conservation practices (e.g. grass-planting, afforestation, check dam) in the WRB from Shaanxi and Gansu Provincial Bureau of Statistics.

Growing season of NDVI in the WRB is the average NDVI from April to September (Shao et al., 2009) since the moderate temperature and concentrated precipitation during that time are favorable for vegetation growth. Besides, monthly and seasonal variation of NDVI were also studied. Spring NDVI was the average monthly NDVI from March to May; summer NDVI was the average monthly NDVI from June to August; and the autumn NDVI was the average monthly NDVI from September to November. Vegetation cover in winter was not investigated because of the influence of snow cover on vegetation and inappropriate condition for vegetation growth.

3. Methodology

3.1. Modified Mann-Kendall trend test method

The Modified Mann-Kendall (MMK) trend test was used to study the monotonic trends in time series. Compared with the Mann-Kendall

Table 1
The information of weather stations of the WRB.

NO.	Weather station	Location		Altitude (m)
		Latitude (°N)	Longitude (°E)	
1	Baoji	34.35	107.13	612
2	Changwu	35.20	107.80	1206
3	Foping	33.52	107.98	827
4	Guyuan	36.00	106.27	1753
5	Huajialing	35.38	105.00	2450
6	Huanxian	36.58	107.30	1255
7	Huashan	34.48	110.08	2064
8	Lintao	35.35	103.85	1893
9	Luochuan	35.82	109.50	1159
10	Minxian	34.43	104.02	2315
11	Pingliang	35.55	106.67	1346
12	Shangzhou	33.87	109.97	742
13	Tianshui	34.58	105.75	1141
14	Tongchuan	35.08	109.07	978
15	Wugong	34.25	108.22	447
16	Wuqi	36.92	108.17	1331
17	Xian	34.30	108.93	397
18	Xifengzhen	35.73	107.63	1421
19	Xiji	35.97	105.72	1916
20	Yanan	36.60	109.50	958
21	Zhenan	33.43	109.15	693

Table 2
The information of hydrological stations of the WRB.

NO.	Hydrological station	Location		Drainage area (km^2)
		Latitude (°N)	Longitude (°E)	
1	Linjiacun	34.38	107.05	30,661
2	Xianyang	34.32	108.70	46,827
3	Huaxian	34.58	109.77	106,498
4	Zhangjiashan	34.63	108.60	43,216
5	Zhuangtou	35.03	109.83	25,645

(MK) trend test, the MMK is good at dealing with serial autocorrelation in time series by considering the lag-*i* autocorrelation (Mann, 1945; Kendall, 1955; Hamed and Rao, 1998). Nowadays, the MMK test is widely adopted to detect trends in hydro-meteorological time series (Daufresne et al., 2009; Huang et al., 2014a,b,c; Liu et al., 2017). More details about this method can be found in Huang et al. (2014b). In this study, the MMK trend test was applied to evaluate the trends in NDVI, precipitation, temperature, SM, runoff and sediment load series across the WRB at the 95% significance level.

3.2. The heuristic segmentation method

The heuristic segmentation method was introduced to detect potential abrupt change point of the NDVI time series.

Given a time series $X = x_1, x_2, \cdots x_{n-1}, x_n$, set a sliding pointer to divide the X into two subseries with one on the left and the other on the right of the pointer, then moves from x_1 to x_{n-1} step by step. $\bar{x}_1$, S_1 and $\bar{x}_2$, S_2 are the mean and standard deviations of these two subseries, respectively. The difference in their means is estimated as:

$$T(i) = \left| \frac{x_1(i) - x_2(i)}{S(i)} \right| \tag{1}$$

$$S(i) = \sqrt{\frac{(n_1 - 1)\cdot S_1 + (n_2 - 1)\cdot S_2}{n - 2} \times \left(\frac{1}{n_1} + \frac{1}{n_2}\right)} \tag{2}$$

where $T(i)$ is the statistic denotes the difference in mean values at i ($1 \le i < n$) position; $S(i)$ is the pooled variance at i position; and n_1, n_2 are the length of left and right subseries, respectively.

The largest T value is taken as a potential change point. Then, the statistical significance $P(t_{\max})$ corresponding to the largest T is defined as follows:

$$P(t_{\max}) \approx \{1 - I_{[\nu/(\nu + t_{\max}^2)]}(\delta\nu, \delta)\}^{\eta} \tag{3}$$

where $\delta = 0.40$, $\nu = n - 2$ and $\eta = 4.19\ln(n) - 11.54$ are derived from the Monte Carlo simulations; and $I_x(a, b)$ refers to the incomplete beta function.

The time series will be cut into two subseries if $P(t_{\max})$ is larger than a threshold of P_0 (ranging from 0.90 to 0.95), and it will continue to iterate until $P(t_{\max})$ is smaller than P_0 or the subseries is shorter than the preset minimum segment length $l_0 (l_0 = 25)$. Otherwise, the time series will not be split.

3.3. The cross wavelet analysis

For two given time series $\{x_n\}$ and $\{y_n\}$, the cross wavelet transform can be used to examine their change characteristics and coupled oscillations both in time and frequency domains (Torrence and Compo, 1998; Huang et al., 2015; 2017). Their cross wavelet transform is expressed as $W^{XY} = W^X W^{Y*}$, where * is their complex conjugation. The cross wavelet power of them is defined as $|W^{XY}|$. The complex argument arg (W^{XY}) is considered as the local relative phase of $\{x_n\}$ and $\{y_n\}$ in time-frequency field. The theoretical distribution of the cross wavelet power between $\{x_n\}$ and $\{y_n\}$ is defined with their background power spectra P_k^X and P_k^Y, as follows:

$$D\left(\frac{W_n^X(s) W_n^{Y*}(s)}{\sigma_X \sigma_Y} < p\right) = \frac{Z_v(p)}{v}\sqrt{P_K^X P_K^Y} \tag{4}$$

where $Z_v(p)$ denotes the significance level connected with the probability p for a probability distribution function defined by the square root of the two χ^2 distributions. The related codes are at http://noc.ac.uk/using-science/crosswavelet-wavelet-coherence.

4. Results

4.1. Changes in vegetation cover at annual scale and in growing season

The MMK trend test was adopted to estimate the long-term trends of annual vegetation cover across the WRB, and the results are displayed in the Fig. 2A. It shows that the WRB is dominated by widespread significant increasing trend of vegetation cover at the 95% confidence level since MMK statistics of annual NDVI in the upstream, the midstream, the downstream, the JRB, and the BRB (this order remains the same in the following) are 3.53, 2.81, 2.81, 2.42 and 2.21, respectively. In general, there is a remarkably irregular spatial distribution of the annual NDVI across the basin as shown in Fig. 2B. Long-term mean annual NDVI of the WRB ranges from 0.33 to 0.58. According to Fig. 2B, the mean annual NDVI in the WRB is relative larger in the lower part of midstream and the whole downstream (most part of the Guanzhong plain), while relatively smaller values exist in other sub-regions of the WRB. The lowest NDVI can be found in the lower reaches of the JRB (part of the Loess Plateau).

Similarly, the MMK statistics of NDVI in the growing season of the five sub-basins are 1.01, 0.99, 2.85, 2.19 and 2.19, respectively, which implies significant increasing trend of vegetation cover in the downstream, the JRB and BRB while insignificant increasing trend of vegetation coverage in the upstream and the midstream in the growing season (Fig. 2C). Besides, vegetation cover of the WRB in growing season also varies greatly, ranging from 0.45 to 0.78, with highest NDVI in the lower reaches of the midstream and smallest NDVI in the lower reaches of the JRB (Fig. 2D). On the whole, vegetation coverage in the WRB exhibits significant increasing trend with the MMK statistics of the whole basin NDVI are 3.53 and 2.29 at annual scale and in growing season, respectively. Overall, the results are consistent with previous studies illustrating increasing trend of “greenness” in many parts of the

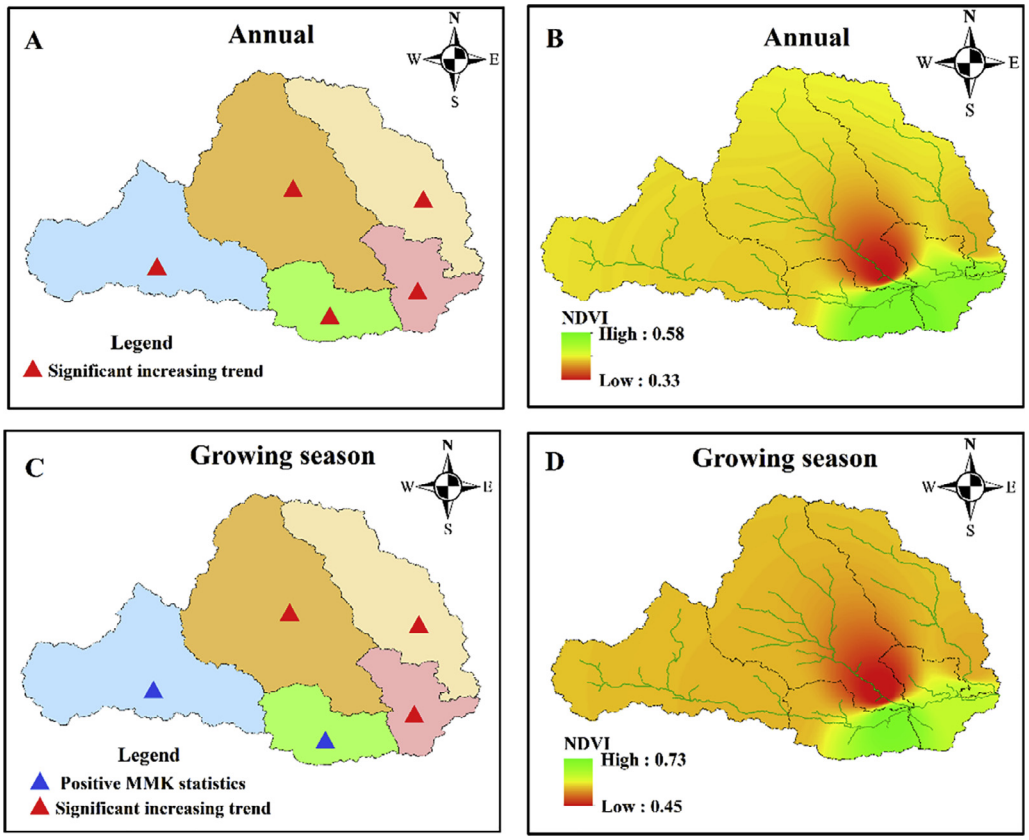

Fig. 2. The MMK statistics of vegetation cover at annual scale and in growing season (A) and (C); and spatial distribution of vegetation cover at annual scale and in growing season (B) and (D), across the WRB. The blue upward triangles denote positive MMK statistics below 95% confidence level. The red upward triangles indicate the statistically significant increasing trend at 95% confidence level.

world (Jong et al., 2011; Piao et al., 2014; Liu and Menzel, 2016; Wen et al., 2016; Gillespie et al., 2018).

4.2. Changes of monthly and seasonal vegetation cover

In order to gain better knowledge of vegetation coverage variation in the WRB during the year, changing patterns of NDVI at monthly and seasonal scales were also examined.

The results of the MMK statistics and spatial distribution of seasonal vegetation cover across the WRB are showed in the Fig. 3. In general, there are significant increasing trends of vegetation coverage in spring and autumn, while no significant trend was detected in summer vegetation cover across the WRB (Fig. 3A, C and E). Specifically, the MMK statistics of NDVI in spring of the five sub-basins are 3.53, 2.81, 2.81, 2.42 and 2.21, respectively, and in autumn are 3.00, 2.59, 3.04, 3.30 and 3.56, respectively. For vegetation in summer, the MMK statistics of NDVI of these five sub-basins are −0.79, −0.51, 0.51, 0.90 and 0.41, respectively, which suggest insignificant decreasing trend of vegetation cover in the upstream and midstream, and insignificant increasing of vegetation coverage in the downstream, the JRB and the BRB. This is in agreement with previous studies which revealed that hotter and drier summer climates would lead to decrease in vegetation cover (Angert et al., 2005; Zhang et al., 2013). When spatial distribution of seasonal NDVI are further considered, the highest value of NDVI mostly appear in the lower reaches of the midstream and smallest NDVI in the lower reaches of the JRB. In addition, with greater NDVI intensity, summer (NDVI ranging from 0.50 to 0.76) tends to be more “greener” than spring (NDVI ranging from 0.29 to 0.59) and autumn (NDVI ranging from 0.34 to 0.57) in the WRB (Fig. 3B, D and F).

Fig. 4 shows the MMK statistics and mean value of monthly vegetation cover at each sub-basins from 1982 to 2010 across the WRB. Significant increasing trends of monthly NDVI are mostly observed in March, April, September, October and November, which might be explained by extended length of growing season caused by warming climate (Li et al., 2016; Fig. 4A). By contrast, significant decreasing trend of monthly NDVI are mainly concentrated in June, July and August, which might account for the decreasing vegetation cover in summer in the upstream and midstream (Fig. 4A). Besides, monthly variation of NDVI in the five sub-basins shows an upside-down U shape distribution over time in general (Fig. 4B). Maximum monthly NDVI are all found in summer (i.e. in July or August), whilst the minimum NDVI of the five sub-basins are all found in winter (i.e. in January or February). Compared to other sub-regions, NDVI intensity of the midstream is largest, and the JRB is smallest, which is in agreement with Fig. 2(B and D) and Fig. 3(B, D and F).

4.3. Change point in annual vegetation cover series

Enhanced human disturbance (e.g., urbanization, deforestation, land use change, and construction of water conservancy projects) and climate change have been observed in the WRB (Huang et al., 2015; Liu et al., 2018b), which might give rise to the abrupt change in annual NDVI time series that may not detected in the overall trend (Wen et al., 2016). Accordingly, the heuristic segmentation method was used to examine the stationarity of annual NDVI time series in the five sub-basins of the WRB. The threshold P_0 was set to 0.95 and minimum segment length ℓ_0 was set to 25.

Fig. 5 is the segmentations and change point in annual NDVI in the upstream. The blue line in Fig. 5 refers to the iteration and segmentation process. Fig. 5 shows that the maximum value of T occurred in 1996, with corresponding $P(t_{\max}) = 0.997 > P_0 = 0.95$. This demonstrates that the year 1996 was a turning point in annual NDVI time series (1982–2010) in the upstream. Since the length of the segments was smaller than ℓ_0, the segmentation process stopped. Based on the same procedures mentioned above, the change points in annual NDVI series in other four sub-regions were also identified, which were summarized in Table 3. Except change point of annual NDVI series of the midstream appeared in 2000, most of the breakpoints occurred in the

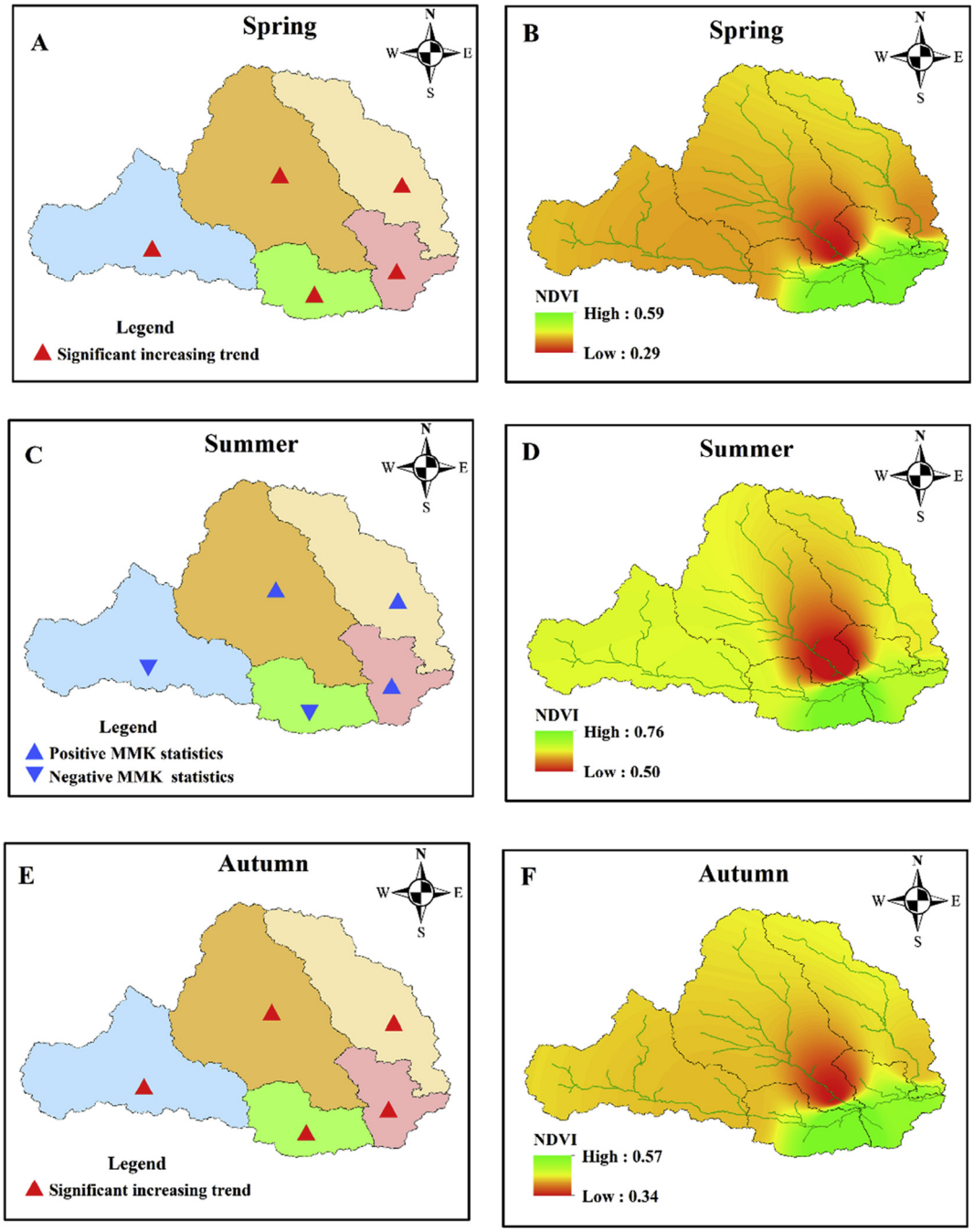

Fig. 3. The same as Fig. 2, but for seasonal vegetation cover across the WRB. The blue upward (downward) triangles denote positive (negative) MMK statistics below 95% confidence level. The red upward triangles indicate the statistically significant increasing trend at 95% confidence level.

mid-1990s: the upstream and the JRB in 1996, the downstream and the BRB in 1995. Hence, the vegetation cover in the basin has considerably changed during the past few decades with significant trends and change points detected in all sub-regions of annual NDVI across the WRB, indicating that the stationarity of annual NDVI series is invalid.

5. Discussion

5.1. Causes of vegetation cover variation in the WRB

In order to find out potential causes for changing vegetation cover in the WRB, the relationship between annual NDVI series and precipitation, temperature and SM series were investigated.

5.1.1. Relationship between NDVI and precipitation

Annual precipitation in the WRB exhibits distinct temporal and spatial patterns (Liu et al., 2017). According to the MMK trend test, there is a dominant but non-significant decreasing trend of precipitation from 1982 to 2010 with the MMK statistics of precipitation of the five sub-basins are −0.84, −0.58, −0.66, −0.58 and −0.77, respectively (Fig. 6).

Fig. 7 is the cross wavelet transforms between precipitation and NDVI in the five sub-basins of the WRB. It shows that precipitation has a statistically significant negative correlation with NDVI series in the upstream with a 4–5 years signal in 1985–1988 (Fig. 7A) at the 95% confidence level. Also, statistically significant negative correlation between precipitation and NDVI series was observed with a signal of 3–5 years from 1983 to 1990 in the midstream and the downstream

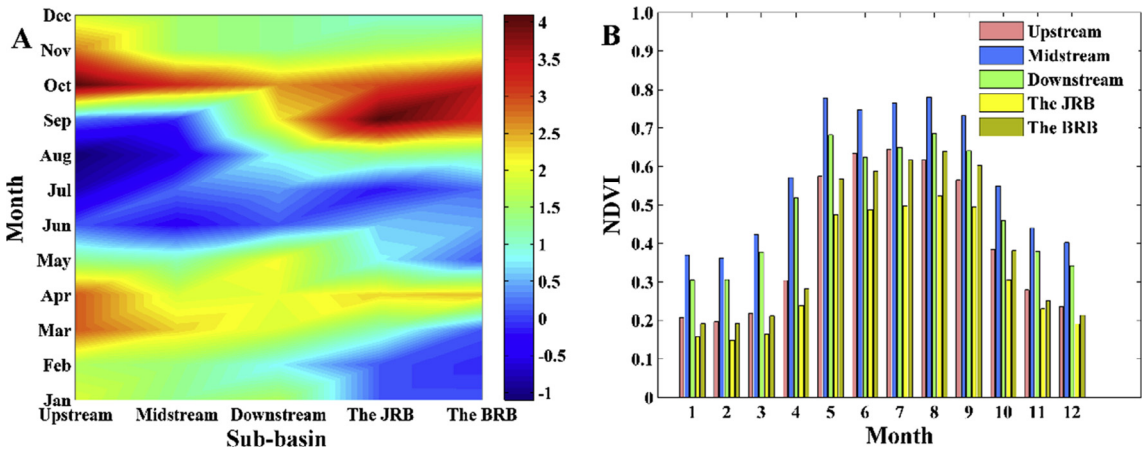

Fig. 4. The MMK statistics (A) and mean value (B) of monthly vegetation cover from 1982 to 2010 at each sub-basin of the WRB.

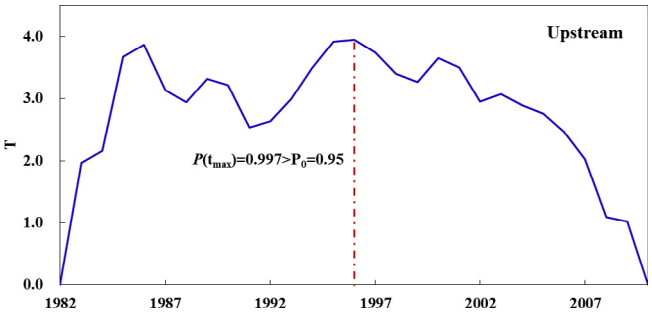

Fig. 5. Segmentation and change point of NDVI in the upstream of the WRB. The blue line refers to the iteration and segmentation process.

Table 3
Change points of annual NDVI in the five sub-regions of the WRB.

Sub-basin	Occurrence time of T_{max}	Corresponding P (t_{max})	Compared to P_0 (=0.95)	Change point
The upstream	1996	0.997	>	1996
The midstream	2000	0.972	>	2000
The downstream	1995	0.998	>	1995
The JRB	1996	0.984	>	1996
The BRB	1995	0.994	>	1995

(Fig. 7B and C). However, no obvious correlation was found between precipitation and NDVI in the JRB, which is consistent with previous study (Fig. 7D; Liu et al., 2018b). For the BRB, precipitation has statistically significant negative correlation with NDVI series with a signal of 3–5 years in 1983–1992 at the 95% confidence level (Fig. 7E). In general, these significant correlations between precipitation and NDVI suggest that, except for the JRB, precipitation plays an important role in the variations of vegetation cover in most parts of the WRB.

5.1.2. Relationship between NDVI and temperature

Similar to vegetation cover in the WRB, there is a significant increasing trend of temperature from 1982 to 2010 at the 95% confidence level with MMK statistics of the five sub-basins are 4.45, 4.22, 4.03, 4.67 and 3.99, respectively (Fig. 6).

Fig. 8 is the cross wavelet transforms between temperature and NDVI in the five sub-basins of the WRB. Obviously, temperature has strong influences on the variations of vegetation coverage across the WRB. Specifically, temperature has a statistically significant positive correlation with NDVI in the upstream with a 2–5 years signal from 1986 to 1992, a 4 years signal from 1993 to 1995, and a 3–4 years signal from 1996 to 2000 at the 95% confidence level (Fig. 8A). Moreover, temperature exhibits a statistically significant positive correlation with the NDVI in the midstream at the 95% confidence level with a 3–5 years signal from 1985 to 1993, a 3–4 years signal from 1994 to 1996, a 2–4 years signal around 1996, a 3–4 years signal from 1997 to 2000, and a 1–2 years signal from 2002 to 2005 (Fig. 8B). For the midstream, statistically significant positive correlation between temperature and NDVI are also found with a 3–5 years signal in 1985–1995 and a 2–4 years signal in 1995–1998 (Fig. 8C). Fig. 8D illustrates that there is a statistically significant positive correlation between temperature and NDVI series in the JRB with a 3.5–4.5 years signal in

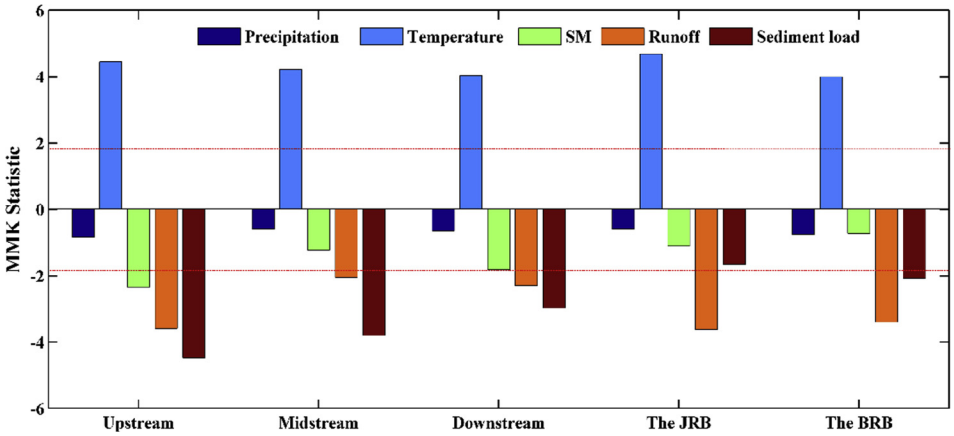

Fig. 6. The MMK trend test results of precipitation, temperature, SM, runoff and sediment load of the five sub-basins of the WRB. The red dash line refers to the 95% significance level (namely, ± 1.96).

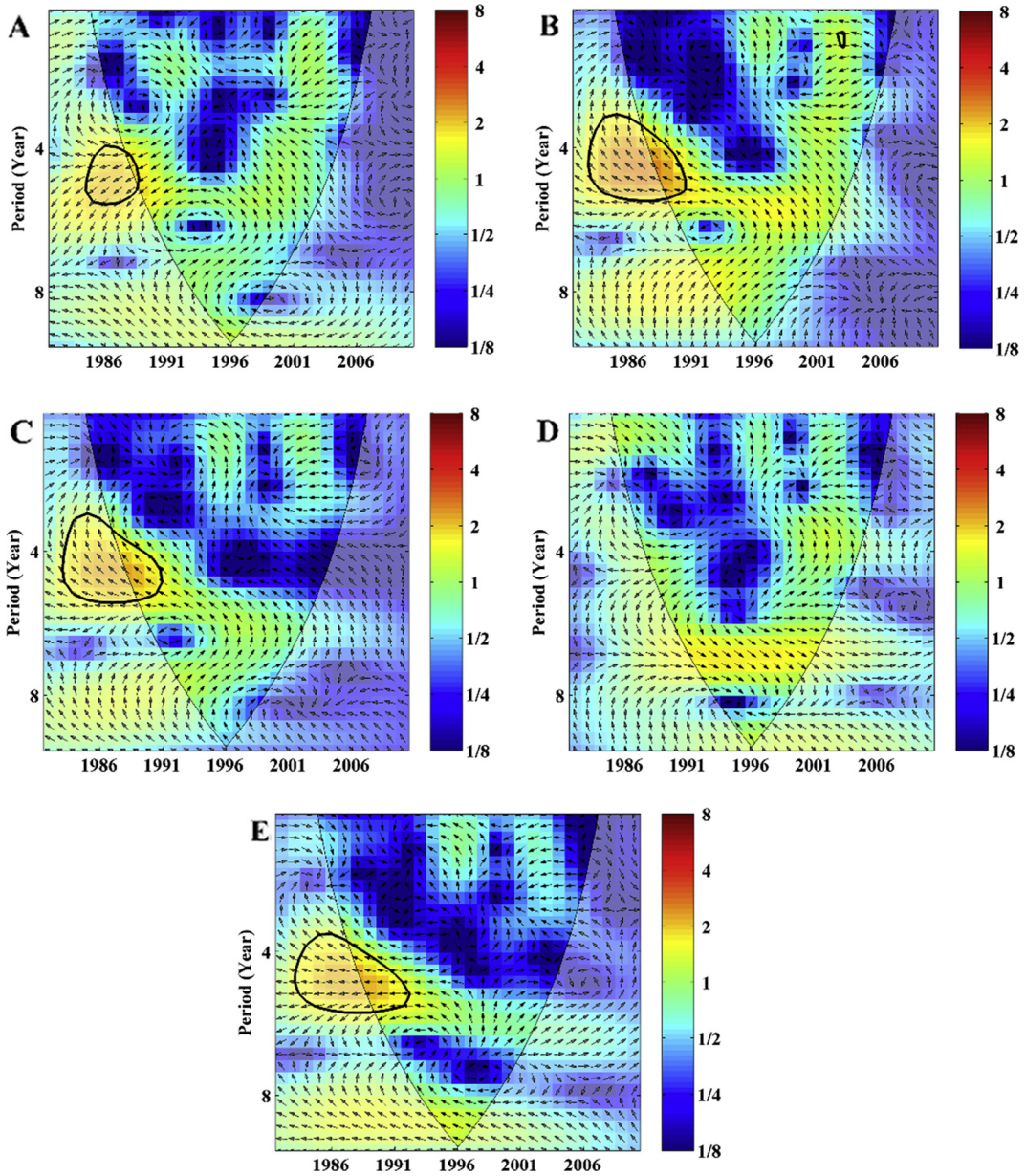

Fig. 7. The cross wavelet transforms between precipitation and NDVI series in the five sub-basins of the WRB: (A) is that of the upstream, (B) is that of the midstream, (C) is that of the downstream, (D) is that of the JRB and (E) is that of the BRB. The 95% significance confidence level against red noise is exhibited as a thick contour, and the relative phase relationship is denoted as arrows (with anti-phase pointing left, in-phase pointing right). The color bar on the right denotes wavelet energy.

1987–1992 and in 1996–1999 at the 95% confidence level. In addition, temperature shows a statistically significant positive correlation with NDVI series in the BRB with a 3–4 years signal from 1986 to 1994, and a 2–4 years signal from 1995 to 1999 at the 95% confidence level (Fig. 8E). Moreover, change points of NDVI in the five sub-basins correspond to the period when temperature is statistically positive correlated with the NDVI series in the five sub-basins, suggesting that temperature has remarkable impacts on the variations of vegetation cover across the WRB.

5.1.3. Connections between NDVI and SM

The MMK statistics of SM of the five sub-basins are −2.34, −1.22, −1.82, −1.11 and −0.73 (Fig. 6), respectively, which implies significant decreasing trend of SM condition in the upstream at the 95% confidence level, and non-significant decreasing trend of SM condition in the other sub-basins of the WRB.

Fig. 9 is the cross wavelet transforms between SM and NDVI in the five sub-basins of the WRB. There is a significant negative correlation between SM and NDVI variations in the upstream at the 95% confidence level, with a 4–5 years signal from 1985 to 1989 and a 1–2 years signal around 2001 (Fig. 9A). SM also has a significant negative correlation with NDVI variations in the midstream at the 95% confidence level, with a 3.5–5 years signal from 1983 to 1991 and a 1–3 years signal from 2001 to 2003 (Fig. 9B). For the downstream, statistically significant negative correlation between SM and NDVI variations was detected with a 3–5 years signal in 1983–1991 at the 95% confidence level (Fig. 9C). Similar relation between SM and NDVI in the BRB has also been found with a 4–5 years signal from 1985 to 1990 (Fig. 9D). However, SM shows a statistically significant positive correlation with NDVI series in the JRB with a 6–6.5 years signal from 1991 to 1998 at the 95% confidence level (Fig. 9E). These findings suggest that variations of vegetation cover in the WRB are also significantly linked to SM.

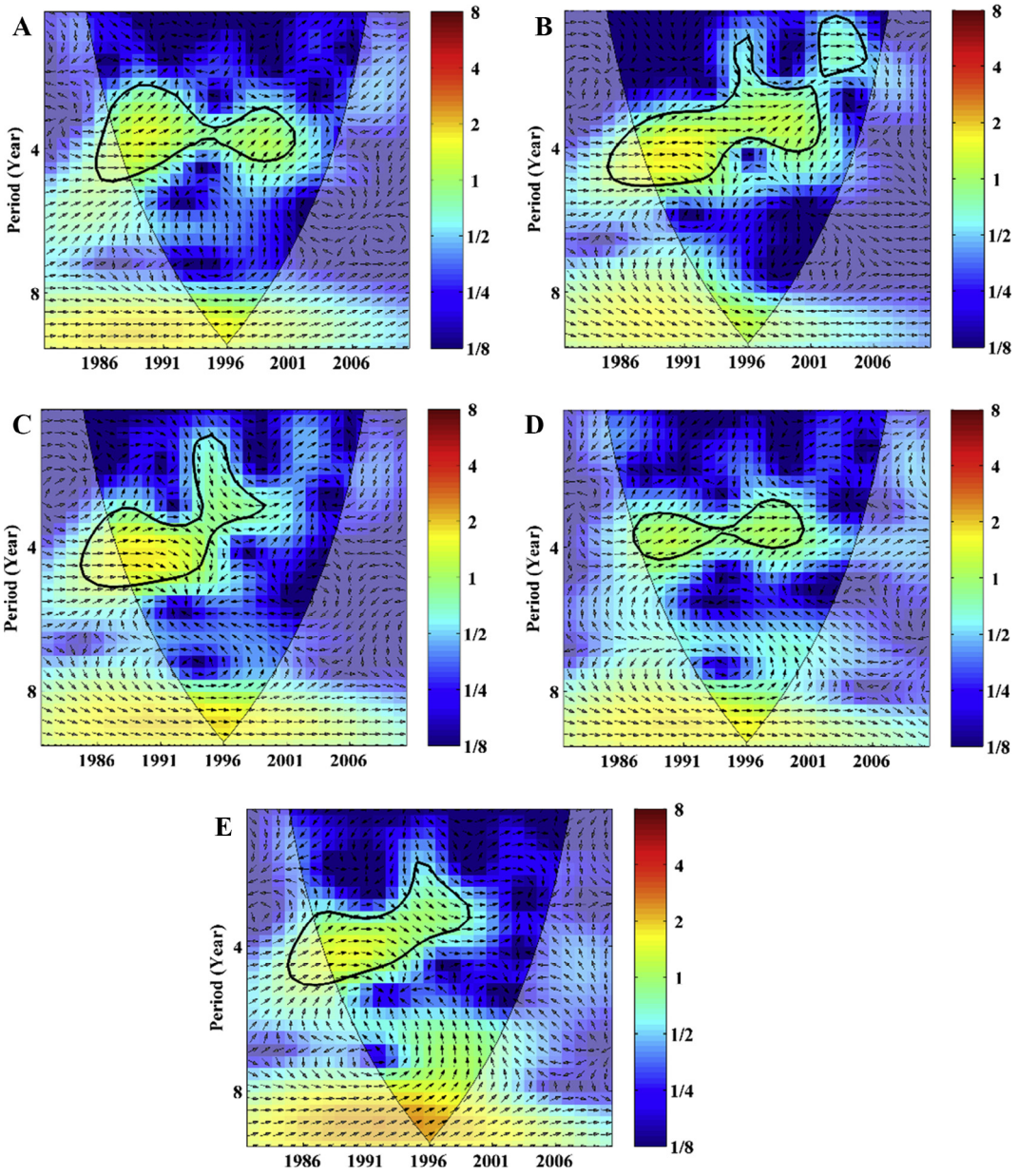

Fig. 8. The same as Fig. 7, but for temperature and NDVI series in the five sub-basins of the WRB.

5.1.4. Causes of increasing vegetation cover in the WRB

To find out the potential climatic factors for significant increase of vegetation cover across the WRB, the relationship between annual NDVI series and precipitation, temperature and SM series of the WRB were investigated. Combining Figs. 7–9, it shows that the relationships between temperature and NDVI are generally the strongest. Moreover, the correlations between SM and NDVI are generally stronger than those of precipitation (Figs. 7–9). To further support these findings, we calculated the correlation coefficients between NDVI and these climatic factors across the basin and results are shown in Fig. 10. Fig. 10 demonstrates that the correlation coefficients between NDVI and temperature is the largest while the coefficients between NDVI and precipitation is the smallest in the WRB.

In general, these findings are consistent with previous studies confirming the influence of temperature on vegetation is more greater than precipitation (e.g. Hou et al., 2015; Liu and Menzel, 2016). As a matter of fact, temperature is important in the growth and development of vegetation which would have effect on the pollination of plants (Bao et al., 2016; Li et al., 2016; Liu et al., 2018b). Although the relationships between temperature and NDVI are strongest among climatic factors, they are different in various sub-regions in both time and frequency domains, which may account for the different spatial change patterns of vegetation coverage across the WRB. As for SM condition, it is more directly associated with dynamics in plant photosynthesis and respiration processes than precipitation (Chen et al., 2014b). Moreover, SM condition is vital in regulating vegetation productivity and controlling terrestrial carbon uptake (Chen et al., 2014b), which might account for stronger relationship between NDVI and SM condition than that between precipitation.

Taking Figs. 7–9 as a whole, the correlations between precipitation, temperature, SM and NDVI are found basically concentrated before the year 2000, and the relationships are weakening after 2000, which means aside from climate change, human activities cannot be neglected. In fact, large-scale ecological restoration projects funded by Chinese Government have been implemented since the 1970s to control soil loss in the WRB. Then two large-scale ecological restoration projects, i.e., the Natural Forest Conservation project and the Grain for Green project, have been launched in 1999 to improve vegetation

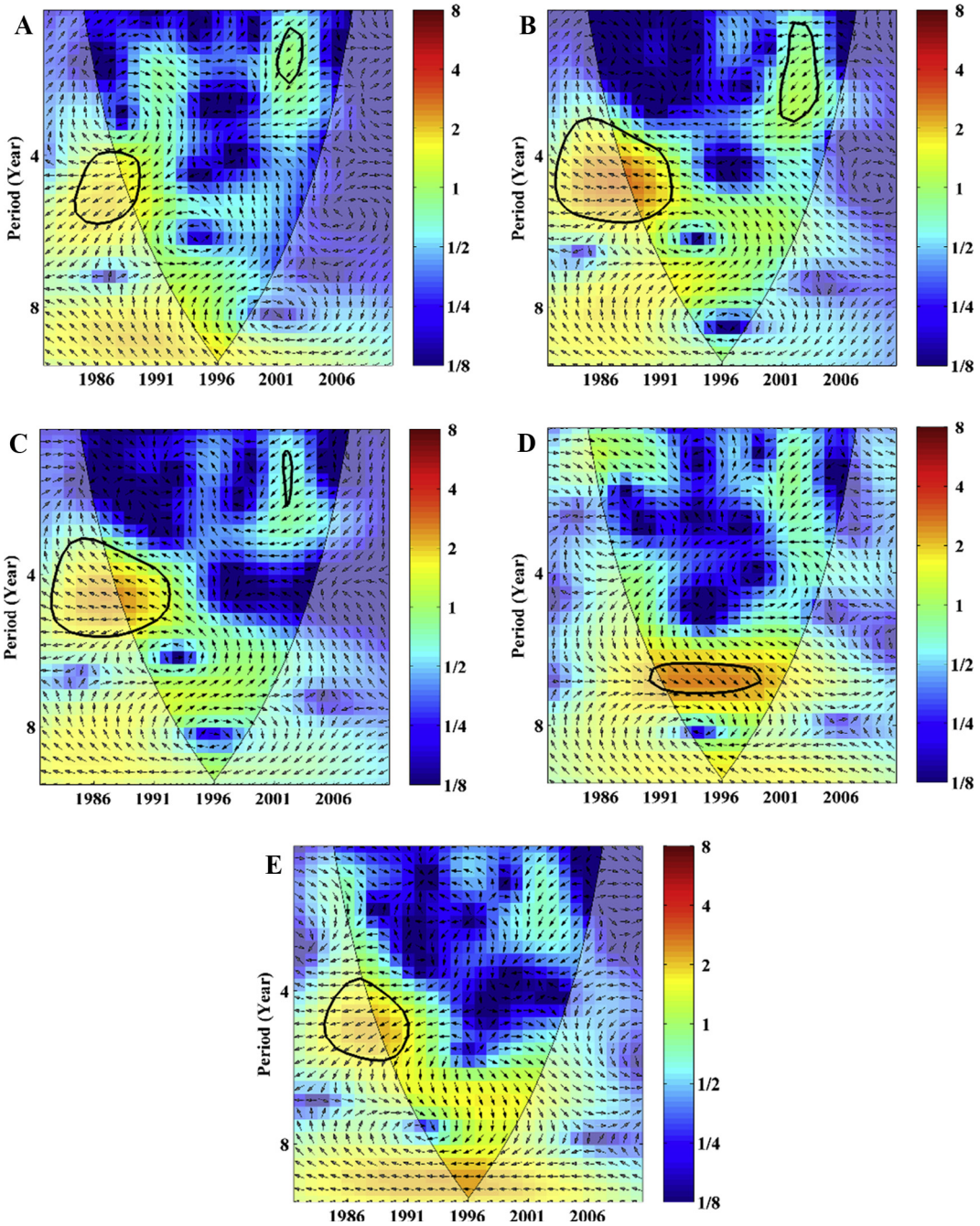

Fig. 9. The same as Fig. 7, but for SM and NDVI series in the five sub-basins of the WRB.

coverage in the WRB, especially in the Loess Plateau (Li et al., 2016). As shown in Fig. 11, the past decades have witnessed remarkable expansion in the area of grass-planting and afforestation from 374 km^2 in 1960 to 21422 km^2 in the 2006 in the WRB. Hence, it can be concluded that increasing vegetation coverage in the WRB is driven by both climate change and human activities. And human activities are expected to be the dominant reasons for vegetation cover increase in the WRB (Li et al., 2016).

5.2. Implications of changing vegetation cover in the WRB

5.2.1. Effects of changing vegetation cover on runoff changes

Contrary to vegetation coverage in the WRB, there is a significant decreasing trend of runoff from 1982 to 2010 at the 95% confidence level with MMK statistic of the five sub-basins are 3.59, −2.04, −2.31, −3.62 and −3.40, respectively (Fig. 6).

Fig. 12 is the cross wavelet transforms between the NDVI and runoff series spanning 1982–2008 across the WRB. It is illustrated that NDVI has a statistically significant negative correlation with runoff series with a signal of 3–5 years in 1988–1988 and a 2–4 years signal in 1989–1990 in the upstream (Fig. 12A). Fig. 12B indicates there is a statistically significant negative correlation between NDVI and runoff series with a 3.5–5 years signal from 1982 to 1991 and 1–2 years signal from 2002 to 2004 in the midstream at the 95% confidence level. For the downstream, there is a statistically significant negative correlation between NDVI and runoff variation with a 3–5 years signal in 1983–1991 at the 95% confidence level (Fig. 12C). However, no obvious relationship was found between NDVI and runoff in the JRB (Fig. 12D). for the BRB, similar relation between NDVI and runoff has also been detected with a signal of 4–5 years from 1983 to 1992

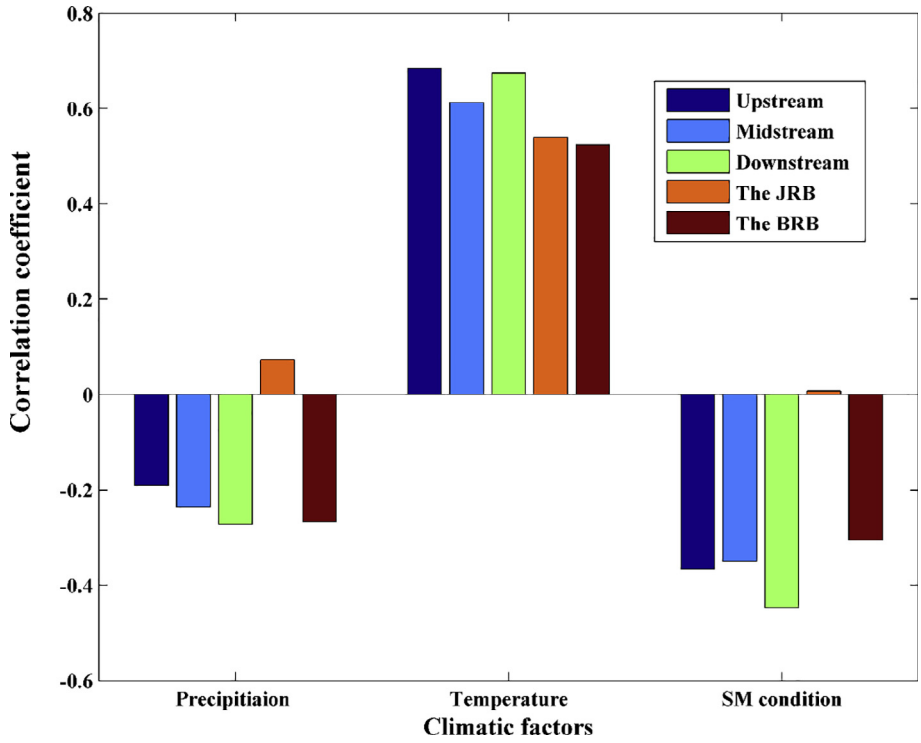

Fig. 10. The correlation coefficients between NDVI series and climatic factors (precipitation, temperature and SM condition) across the WRB.

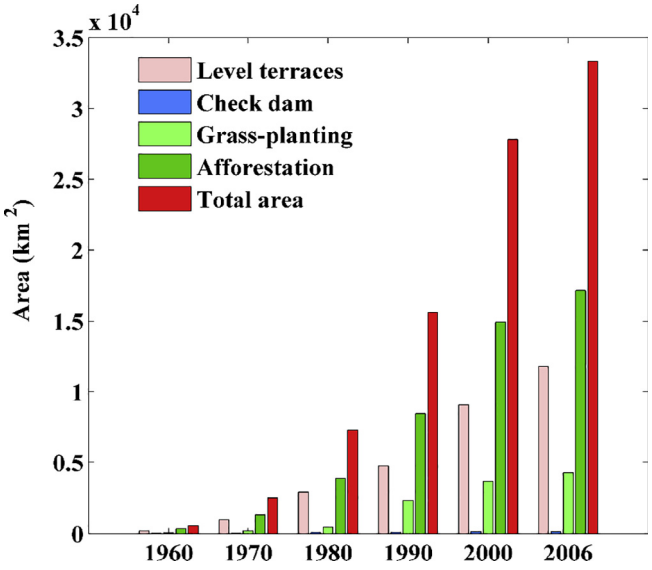

Fig. 11. Accumulative area of different soil conservation practices in the WRB from 1960 to 2006.

(Fig. 12E). In general, these correlations suggest that increasing vegetation cover would impact the reduction of runoff in the WRB.

5.2.2. Effects of changing vegetation cover on sediment load changes

Annual average sediment transported into the five sub-basins of the WRB during 1982–2010 are roughly 0.52×10^8t, 0.47×10^8t, 2.20×10^8t, 1.80×10^8t and 0.57×10^8t, respectively. The trend test shows that, except for the JRB, there is a significant decreasing trend of sediment discharge in the WRB at the 95% confidence level with MMK statistic of the five sub-basins are −4.48, −3.81, −2.98, −1.67 and −2.08, respectively (Fig. 6).

Fig. 13 is the cross wavelet transform between NDVI and sediment load series in the five sub-basins of the WRB. It is demonstrated that the NDVI has a statistically significant negative correlation with the sediment load variations in the upstream with a 2–4 years signal from 1986 to 1991 and a 2 years signal around 1992 to 1993 at the 95% confidence level (Fig. 13A). Also, there is a statistically significant negative correlation between NDVI and sediment load series in the midstream with a 2–4 years signal in 1986–1991 and a 1–3 years signal from 2001 to 2004 (Fig. 13B). For the downstream, NDVI shows a statistically significant negative correlation with sediment load with a 3–5 years signal in 1984–1911 (Fig. 13C). By comparison, there is no correlation between NDVI and sediment load in the JRB (Fig. 13D). For the BRB, NDVI exhibits statistically significant negative correlation with sediment load with a 2–3 year signal in 1994–1997 (Fig. 13E). These correlations indicate that increasing vegetation coverage plays an important role in affecting the sediment load changes, thereby influencing local soil and water conservation.

5.2.3. Causes for reduced runoff and sediment load in the WRB

In contrast to increasing vegetation coverage across the basin, there is a dominant significant decreasing trends of runoff and sediment in the WRB. Similar to the correlations between NDVI and different climatic factor, the relationships between NDVI and runoff, sediment are mostly concentrated before the year 2000 (Figs. 12 and 13), suggesting increasing vegetation cover might be the reason for reduction of runoff and sediment to some extent. Whilst large-scale human activities, including hyper-irrigation and water and soil conservation, are the direct reason for the decrease of runoff and sediment load in the WRB (Chang et al., 2015). It was reported that the irrigated areas in the WRB have reached about 9500 km^2 in 2008 due to the development of economy and increasing population with large amounts of water diverted from the JRB and WRB (Chang et al., 2015; Liu et al., 2018b). Decreasing runoff in the river lowered the sediment carrying capacity and further reduced sediment discharge. Fig. 11 shows the accumulative area of different soil conservation practices in the WRB from 1960 to 2006. In the past decades, the soil conservation area in the WRB has expanded tens-fold from 552 km^2 in 1960 to 33344 km^2 in 2006 (Fig. 11), which effectively reduced sediment load in the river. Meanwhile, these soil conservation practices would reduce runoff by changing local

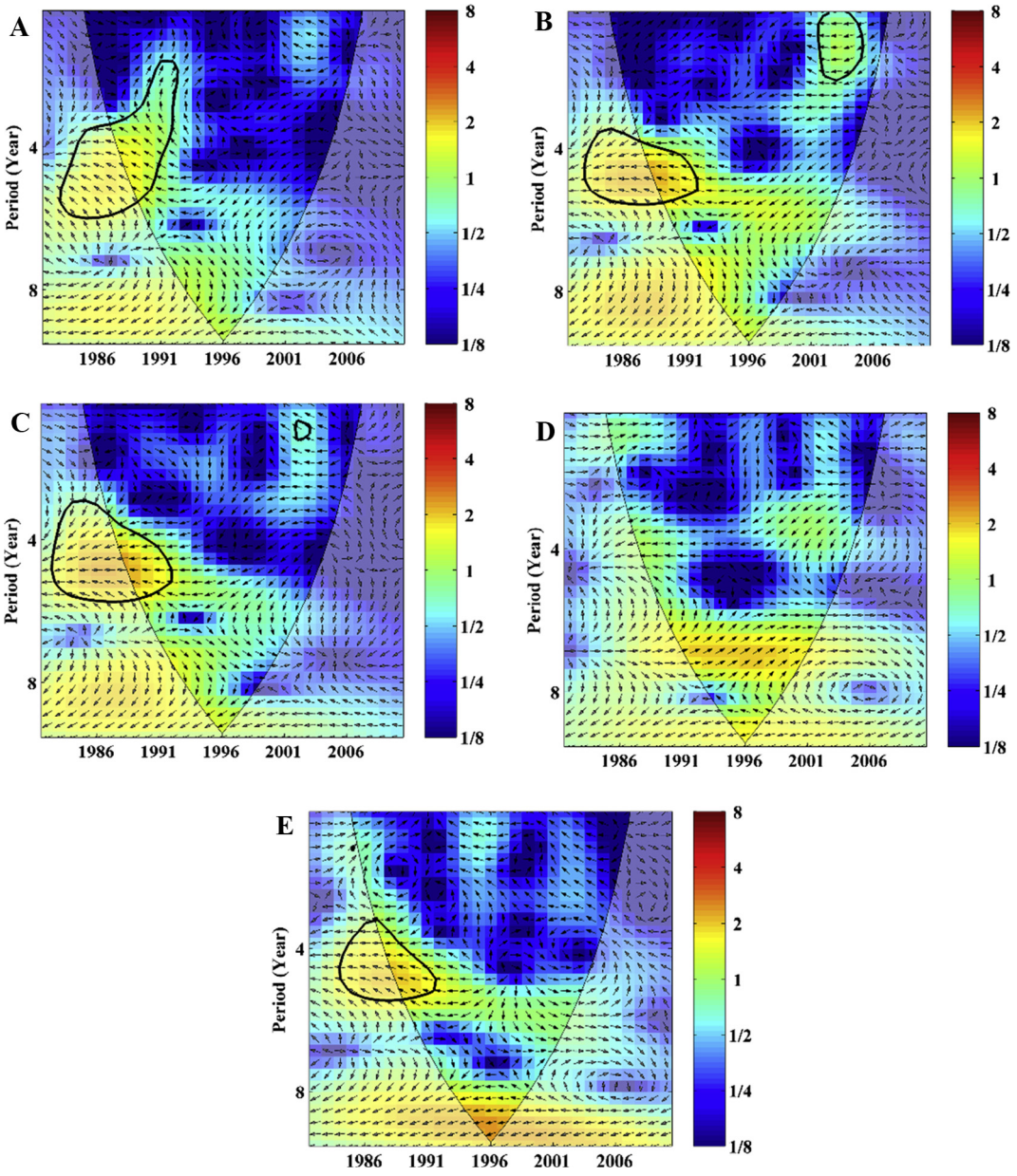

Fig. 12. The same as Fig. 7, but for NDVI and runoff series in the five sub-basins of the WRB.

microtopography, intercepting precipitation, impeding overland flow and increase infiltrating time (Chang et al., 2015; Duan et al., 2016). Hence, both vegetation cover and human activities lead to the reduction of runoff and sediment discharge in the WRB.

5.2.4. What should we do with increasing vegetation cover

In order to control soil loss in the Loess Plateau, Chinese Government have made great effort to carry out large-scale ecological restoration projects since the 1970s by planting grass, afforestation, which lead to increasing vegetation cover in the WRB (part of the Loess Plateau). At present, these projects begun to highlight its ecological effects. According to the study of Liu et al. (2016), evapotranspiration increased significantly due to the vegetation recovery strategies and resulted in the decrease of runoff, which further support our findings. However, Liu et al. (2016) argued it has reached a relative stable state between the hydrothermal and vegetation conditions. If we keep the status quo, the water consumption of forest and grass will be maintained at a relative level and will fluctuate associated with precipitation (Liu et al., 2016). Otherwise, if we continue to adopt the large-scale ecological measures, new problems will inevitably arise since there is enhanced evapotranspiration while reduced renewability of runoff (Xin et al., 2009). Therefore, confronted with increasing vegetation cover, it is worthwhile to study the potential influences of large-scale ecological restoration projects on water supply security and the balance of erosion and sedimentation in the Yellow River Delta and to determine the reasonable project scale.

6. Conclusions

Investigation of vegetation coverage is of important significance to monitor terrestrial ecosystem evolution and to guide regional environmental management under changing environments. In this study, we focused on vegetation cover in the WRB, a typical eco-environmentally vulnerable region in the Loess Plateau, China.

Our results show significant increasing trends of vegetation cover (indexed by NDVI) at annual scale and in growing season. However, the stationarity of annual NDVI series is invalid with change points identified in all sub-regions of the WRB.

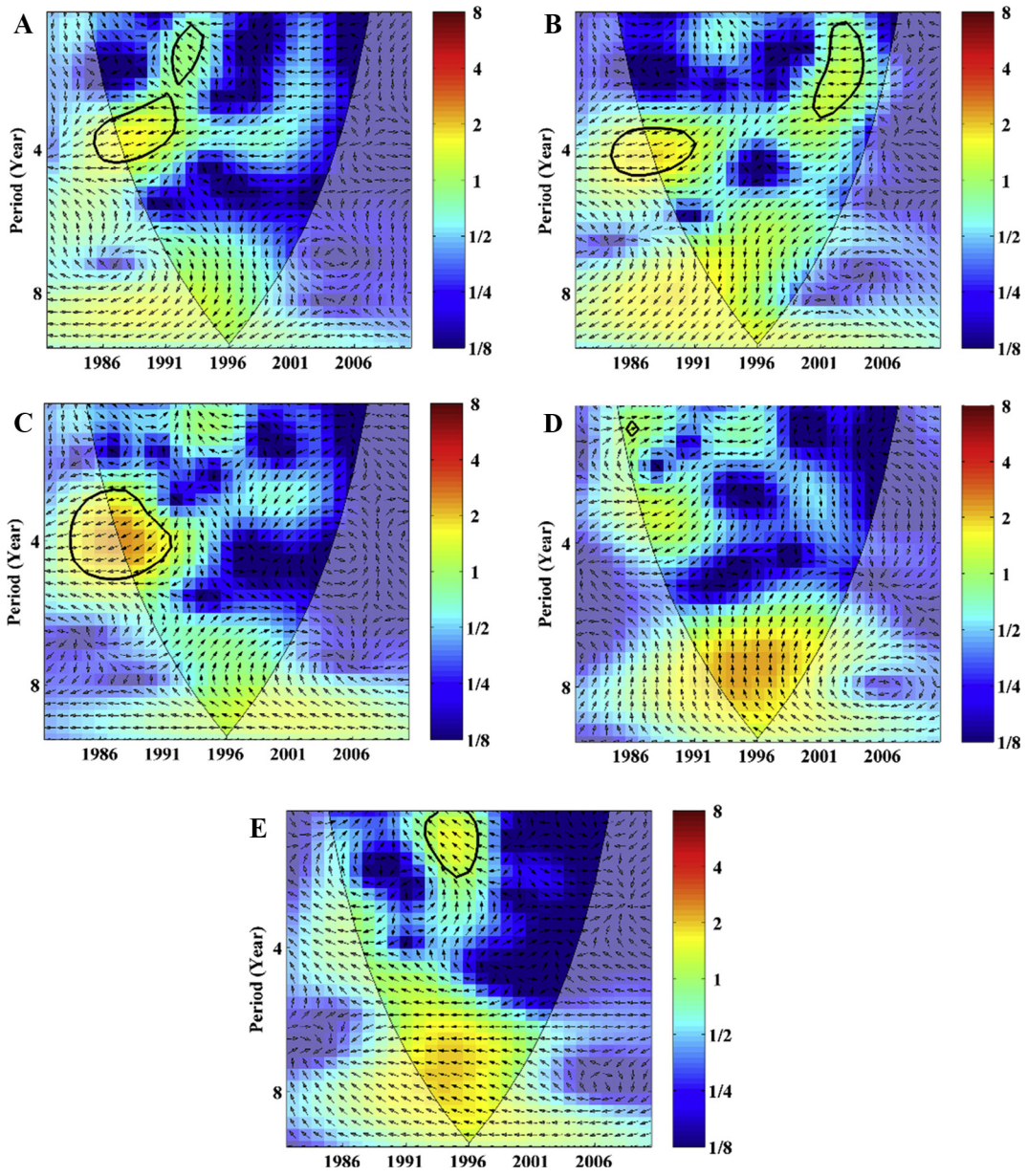

Fig. 13. The same as Fig. 7, but for NDVI and sediment load series in the five sub-basins of the WRB.

Significant increasing vegetation cover in the WRB are more influenced by temperature and SM condition than precipitation. Moreover, human activities including glass-planting and afforestation also contributes to vegetation cover increase in the WRB. Increasing vegetation cover is found responsible for the reduction of runoff and sediment to some extent. Therefore, runoff and sediment into the YRB would be further reduced with expansion of the ecological restoration project in the future in the Loess Plateau, which would negatively influence local water supply and the balance of erosion and deposition in the Yellow River Delta. Therefore, it is very necessary to deal with the relationship between the scale of the ecological restoration project and local water supply and the balance of erosion and deposition in the Yellow River Delta for the department concerned.

Acknowledgements

This research was supported by the National Natural Science Foundation of China (51709221), the Planning Project of Science and Technology of Water Resources of Shaanxi (2015slkj-27; 2017slkj-19), National Key R&D Program of China (2017YFC0405900), Key laboratory research projects of education department of Shaanxi province (17JS104), China Scholarship Council (201708610118), and the Open Research Fund of State Key Laboratory of Simulation and Regulation of Water Cycle in River Basin (China Institute of Water Resources and Hydropower Research) (IWHR-SKL-KF201803).

References

Angert, A., Biraud, S., Bonfils, C., et al., 2005. Drier summers cancel out the CO_2 uptake enhancement induced by warmer springs. PNAS 102 (31), 10823–10827.
Bao, G., Bao, Y., Sanjjava, A., et al., 2016. NDVI-indicated long-term vegetation dynamics in Mongolia and their response to climate change at biome scale. Int. J. Climatol. 35 (14), 4293–4306.
Begue, A., Vintrou, E., Ruelland, D., et al., 2011. Can a 25-year trend in Soudano-Sahelian vegetation dynamics be interpreted in terms of land use change? A remote sensing approach. Glob. Environ. Chang. 21, 413–420.
Cao, R., Jiang, W., Yuan, L., et al., 2014. Inter-annual variations in vegetation and their response to climatic factors in the upper catchments of the Yellow River from 2000 to 2010[J]. J. Geog. Sci. 24 (6), 963–979.
Chang, J., Wang, Y., Istanbulluoglu, E., et al., 2015. Impact of climate change and human activities on runoff in the Weihe River Basin, China. Quat. Int. 380–381, 169–179.

Chen, T., De, J.R.A.M., Liu, Y.Y., et al., 2014b. Using satellite based soil moisture to quantify the water driven variability in NDVI: A case study over mainland Australia. Remote Sens. Environ. 140 (140), 330–338.
Chen, J., Luo, Y., Xia, J., et al., 2016. Differential responses of ecosystem respiration components to experimental warming in a meadow grassland on the Tibetan Plateau. Agric. For. Meteorol. 220, 21–29.
Chen, J., Luo, Y., Xia, J., et al., 2018. Divergent responses of ecosystem respiration components to livestock exclusion on the Qinghai Tibetan Plateau. Land Degrad. Dev. 29, 1726–1737.
Chen, B., Xu, G., Coops, N.C., et al., 2014a. Changes in vegetation photosynthetic activity trends across the Asia-Pacific region over the last three decades. Remote Sens. Environ. 144, 28–41. https://doi.org/10.1016/j.rse.2013.12.018.
Daufresne, M., Lengfellner, K., Sommer, U., 2009. Global warming benefits the small in aquatic ecosystems. Proceedings of the National Academy of Sciences USA 106 (31), 12788–12793.
Duan, L., Huang, M., Zhang, L., 2016. Differences in hydrological responses for different vegetation types on a steep slope on the Loess Plateau. China. Journal of Hydrology 537 (537), 356–366.
Fang, W., Huang, Q., Huang, S., et al., 2017. Optimal Sizing of Utility-scale Photovoltaic Power Generation Complementarily Operating with Hydropower: A Case Study of the World's Largest Hydro-photovoltaic Plant. Energy Convers. Manage. 136, 161–172.
Fang, W., Huang, S., Huang, Q., et al., 2018. Reference evapotranspiration forecasting based on local meteorological and global climate information screened by partial mutual information. J. Hydrol. 561, 764–779.
Fang, W., Huang, S.Z., Ren, K., et al., 2019. Examining the applicability of different sampling techniques in the development of decomposition-based streamflow forecasting models. J. Hydrol (in press).
Gillespie, T.W., Ostermann-Kelm, S., Dong, C., et al., 2018. Monitoring changes of NDVI in protected areas of southern California. Ecol. Ind. 88, 485–494.
Guo, A., Chang, J., Wang, Y., et al., 2018. Flood risk analysis for flood control and sediment transportation in sandy regions: a case study in the Loess Plateau, China. J. Hydrol. 560, 39–55.
Hamed, K.H., Rao, A.R., 1998. A modified Mann-Kendall trend test for autocorrelated data. J. Hydrol. 204 (1–4), 182–196.
Hou, W., Gao, J., Wu, S., et al., 2015. Interannual Variations in Growing-Season NDVI and Its Correlation with Climate Variables in the Southwestern Karst Region of China. Remote Sensing 7 (9), 11105–11124.
Huang, S., Chang, J., Huang, Q., et al., 2014b. Spatio-temporal changes and frequency analysis of drought in the Wei River Basin. China. Water Resources Management 28 (10), 3095–3110.
Huang, S., Chang, J., Huang, Q., et al., 2014c. Monthly streamflow prediction using modified EMD-based support vector machine. J. Hydrol. 511, 764–775.
Huang, S., Chang, J., Huang, Q., Wang, Y., Hirano, S., Masuda, N., Oda, H., et al., 2014a. Spatio-temporal changes in potential evaporation based on entropy across the Wei River Basin. Water Resour. Manage. 28 (13), 4599–4613.
Huang, S., Huang, Q., Chang, J., et al., 2015. Drought structure based on a nonparametric multivariate standardized drought index across the Yellow river basin, China. J. Hydrol. 530, 127–136.
Huang, S., Huang, Q., Chang, J., et al., 2016. Linkages between hydrological drought, climate indices and human activities: a case study in the Columbia River basin. Int. J. Climatol. 36 (1), 280–290.
Huang, S., Huang, Q., Leng, G., et al., 2017. Variations in annual water-energy balance and their correlations with vegetation and soil moisture dynamics: A case study in the Wei River Basin, China. J. Hydrol. 546, 515–525.
Jia, X., Shao, M., Zhu, Y., et al., 2017. Soil moisture decline due to afforestation across the Loess Plateau, China. J. Hydrol. 546, 113–122.
Jong, R.D., Bruin, S.D., Wit, A.D., et al., 2011. Analysis of monotonic greening and browning trends from global NDVI time-series. Remote Sens. Environ. 115 (2), 692–702.
Kendall, M.G., 1955. Rank Correlation Methods. Griffin, London.
Lei, H., Yang, D., Huang, M., 2014. Impacts of climate change and vegetation dynamics on runoff in the mountainous region of the Haihe River basin in the past five decades. J. Hydrol. 511 (4), 786–799.
Li, S., Liang, W., Fu, B., et al., 2016. Vegetation changes in recent large-scale ecological restoration projects and subsequent impact on water resources in China's Loess Plateau. Science of the Total Environment, s 569–570, 1032–1039.
Liu, S., Huang, S., Huang, Q., et al., 2017. Identification of the non-stationarity of extreme precipitation events and correlations with large-scale ocean-atmospheric circulation patterns: A case study in the Wei River Basin, China. J. Hydrol. 548, 184–195.
Liu, S., Huang, S., Xie, Y., et al., 2018a. Spatial-temporal changes of rainfall erosivity in the loess plateau, China: Changing patterns, causes and implications. Catena 166, 279–289.
Liu, S., Huang, S., Xie, Y., et al., 2018b. Spatial-temporal changes of maximum and minimum temperatures in the Wei River Basin, China: Changing patterns, causes and implications. Atmos. Res. 204, 1–11.
Liu, C., Li, Y., Liu, X., et al., 2016. Impact of Vegetation Change on Water Transformation in the Middle Yellow River. Yellow River 38 (10), 7–12 (in Chinese).
Liu, Z., Menzel, L., 2016. Identifying long-term variations in vegetation and climatic variables and their scale-dependent relationships: A case study in Southwest Germany. Global Planet. Change 147, 54–66.
Mann, H.B., 1945. Nonparametric tests against trend. Econometrica 13, 245–259.
Meng, E.H., Huang, S.Z., Huang, Q., et al., 2019. A robust method for non-stationary streamflow prediction based on improved EMD-SVM model. J. Hydrol (in press).
Pang, G., Wang, X., Yang, M., 2016. Using the NDVI to identify variations in, and responses of, vegetation to climate change on the Tibetan Plateau from 1982 to 2012. Quat. Int. 444, 87–96.
Piao, S., Nan, H., Huntingford, C., et al., 2014. Evidence for a weakening relationship between interannual temperature variability and northern vegetation activity. Nat. Commun. 5, 5018.
Reynolds, J.F., Smith, D.M., Lambin, E.F., et al., 2007. Global desertification: building a science for dryland development. Science 2007 (316), 847–851.
Shao, W., Yang, D., Sun, F., et al., 2009. Relationship between vegetation cover and water balance in the Loess Plateau. Tsinghua Sci. Technol. 49 (12), 1958–1962 (in Chinese).
Torrence, C., Compo, G.P., 1998. A Practical Guide to Wavelet Analysis. Bull. Am. Meteorol. Soc. 79, 61–78.
Wang, J., Rich, P.M., Price, K.P., 2003. Temporal responses of NDVI to precipitation and temperature in the central Great Plains. USA. International Journal of Remote Sensing 24 (11), 2345–2364.
Wen, Z., Wu, S., Chen, J., et al., 2016. NDVI indicated long-term interannual changes in vegetation activities and their responses to climatic and anthropogenic factors in the Three Gorges Reservoir Region, China. Sci. Total Environ. 574, 947–959.
Xin, Z., Yu, X., Gan, J., et al., 2009. Vegetation restoration and its effects on runoff and sediment yield in Hekouzhen-Longmen Section of the middle reaches of Yellow River. Journal of Beijing Forestry University 31 (5), 1–7 (in Chinese).
Zewdie, W., Csaplovics, E., Inostroza, L., 2017. Monitoring ecosystem dynamics in northwestern Ethiopia using NDVI and climate variables to assess long term trends in dryland vegetation variability. Appl. Geogr. 79, 167–178.
Zhang, W., An, S., Xu, Z., et al., 2011. The impact of vegetation and soil on runoff regulation in headwater streams on the east Qinghai-Tibet Plateau. China. Catena 87 (2), 182–189.
Zhang, Y., Gao, J., Liu, L., et al., 2013. NDVI-based vegetation changes and their responses to climate change from 1982 to 2011: A case study in the Koshi River Basin in the middle Himalayas. Global Planet. Change 108 (108), 139–148.
Zhang, L., Wang, J., Bai, Z., et al., 2015. Effects of vegetation on runoff and soil erosion on reclaimed land in an opencast coal-mine dump in a loess area. Catena 128, 44–53.
Zheng, F., 2006. Effect of Vegetation Changes on Soil Erosion on the Loess Plateau. Pedosphere 16 (4), 420–427.